NGRIP CH4 concentration from 120 to 10 kyr before present and its relation to a δ15N temperature reconstruction from the same ice core

M. Baumgartner, P. Kindler, O. Eicher, G. Floch, A. Schilt, J. Schwander, R. Spahni, E. Capron, J. Chappellaz, M. Leuenberger, et al.

Clim. Past, 10, 903–920, 2014
www.clim-past.net/10/903/2014/
doi:10.5194/cp-10-903-2014

Climate of the Past
Open Access

NGRIP CH_4 concentration from 120 to 10 kyr before present and its relation to a $\delta^{15}N$ temperature reconstruction from the same ice core

M. Baumgartner[1], P. Kindler[1], O. Eicher[1], G. Floch[2,3], A. Schilt[1], J. Schwander[1], R. Spahni[1], E. Capron[4,5], J. Chappellaz[2,3], M. Leuenberger[1], H. Fischer[1], and T. F. Stocker[1]

[1]Climate and Environmental Physics, Physics Institute, and Oeschger Centre for Climate Change Research, University of Bern, Sidlerstrasse 5, 3012 Bern, Switzerland
[2]CNRS, Laboratoire de Glaciologie et Géophysique de l'Environnement (LGGE), 38041 Grenoble, France
[3]Univ. Grenoble Alpes, Laboratoire de Glaciologie et Géophysique de l'Environnement (LGGE), 38041 Grenoble, France
[4]British Antarctic Survey, NERC, High Cross, Madingley Road, Cambridge, CB3 0ET, UK
[5]Insitut Pierre-Simon Laplace/Laboratoire des Sciences du Climat et de l'Environnement, UMR8212, CEA-CNRS-UVSQ, 91191 Gif-sur-Yvette, France

Correspondence to: M. Baumgartner (baumgartner@climate.unibe.ch)

Received: 11 July 2013 – Published in Clim. Past Discuss.: 14 August 2013
Revised: 23 February 2014 – Accepted: 9 March 2014 – Published: 30 April 2014

Abstract. During the last glacial cycle, Greenland temperature showed many rapid temperature variations, the so-called Dansgaard–Oeschger (DO) events. The past atmospheric methane concentration closely followed these temperature variations, which implies that the warmings recorded in Greenland were probably hemispheric in extent. Here we substantially extend and complete the North Greenland Ice Core Project (NGRIP) methane record from the Preboreal Holocene (PB) back to the end of the last interglacial period with a mean time resolution of 54 yr. We relate the amplitudes of the methane increases associated with DO events to the amplitudes of the local Greenland NGRIP temperature increases derived from stable nitrogen isotope ($\delta^{15}N$) measurements, which have been performed along the same ice core (Kindler et al., 2014). We find the ratio to oscillate between 5 parts per billion (ppb) per °C and 18 ppb °C^{-1} with the approximate frequency of the precessional cycle. A remarkably high ratio of 25.5 ppb °C^{-1} is reached during the transition from the Younger Dryas (YD) to the PB. Analysis of the timing of the fast methane and temperature increases reveals significant lags of the methane increases relative to NGRIP temperature for DO events 5, 9, 10, 11, 13, 15, 19, and 20. These events generally have small methane increase rates and we hypothesize that the lag is caused by pronounced northward displacement of the source regions from stadial to interstadial. We further show that the relative interpolar concentration difference (rIPD) of methane is about 4.5 % for the stadials between DO events 18 and 20, which is in the same order as in the stadials before and after DO event 2 around the Last Glacial Maximum. The rIPD of methane remains relatively stable throughout the full last glacial, with a tendency for elevated values during interstadial compared to stadial periods.

1 Introduction

Methane (CH_4) is a potent greenhouse gas with preindustrial atmospheric concentrations changing between 350 and 750 ppb over the last 800 thousand years (kyr) (Loulergue et al., 2008). This statement is based on measurements on polar ice cores, a unique archive to reconstruct the past atmospheric composition. Human activity has increased the atmospheric abundance of CH_4 from the preindustrial Holocene level of 750 ppb to around 1800 ppb over the last 200 yr (Hartmann et al., 2013). The increase rate under the anthropogenic influence peaked around 1981 at 17 ppb yr^{-1} (Etheridge et al., 1998). Ice core measurements over the last

glacial cycle revealed numerous fast and strong variations in the CH_4 concentration, when only natural sources have been present. However, the maximum increase rate observed alongside DO events during the last glaciation and deglaciation of up to 2.5 ppb yr^{-1} (Chappellaz et al., 2013) is far below the maximum increase rate under the anthropogenic influence. Although atmospheric CH_4 concentrations can be readily measured using polar ice cores, important questions concerning the location and strength of the different sources and sinks, and the sensitivity of the emissions to climate change, are still open.

The major natural sources of CH_4 are wetlands (Spahni et al., 2011), where archaea produce CH_4 by the degradation of organic material under anaerobic conditions (e.g., Bridgham et al., 2013). The absence of molecular oxygen is crucial for methanogenesis, underlining the importance of water in the source regions acting as a gas barrier. Precipitation determines wetland extent and water saturation of the soil and thus strongly influences the global CH_4 source strength (Bloom et al., 2010). Given anoxic conditions in wetland areas the CH_4 production rate generally increases with increasing temperature (Christensen et al., 2003; Walter et al., 2001; Ringeval et al., 2013; Zürcher et al., 2013). Bottom-up models of CH_4 emission further suggest that net primary productivity regulates the carbon pool available for methanogenesis, and thus CH_4 production and emissions (Melton et al., 2013; Wania et al., 2013). After its emission, CH_4 is mixed in the global atmosphere within a few years, leading to a relatively uniform concentration distribution. Under present day conditions its atmospheric lifetime is 9.1 ± 0.9 yr (Prather et al., 2012), controlled by oxidation in the troposphere by its major sink, the OH radical. We assume a minor influence of variations in the sink strength to the atmospheric CH_4 budget during the last glacial cycle, in line with recent results of atmospheric chemistry modeling studies (Levine et al., 2011, 2012). Both the strongest source and sink strengths are found in the tropical regions, but boreal wetlands also contribute substantially to the global emissions (Spahni et al., 2011). The Northern Hemisphere dominates the emissions due to its larger land area compared to the Southern Hemisphere, which leads to asymmetry of the latitudinal source distribution and to an interpolar concentration difference also documented by bipolar ice core studies (e.g., Baumgartner et al., 2012; Brook et al., 2000; Chappellaz et al., 1997).

During the last glacial cycle, Greenland temperature experienced many rapid and strong variations (NGRIP Project Members, 2004), the so-called DO events (Dansgaard et al., 1982). While the northward heat transport by the Atlantic Meridional Overturning Circulation (AMOC) plays a key role in producing such variations (Capron et al., 2010a; McManus et al., 2004; Piotrowski et al., 2004; Stocker and Johnsen, 2003), more regional processes, such as the sudden collapse of the sea ice coverage in the Nordic Sea, may also contribute to the amplitude and speed of the changes (Li et al., 2010; Petersen et al., 2013). It has been shown that the correlation between Greenland temperature and CH_4 concentration is extraordinarily strong (Huber et al., 2006; Brook et al., 1996) and that therefore the warmings recorded in Greenland are mirrored by changes in a larger portion of the Northern Hemisphere (Voelker, 2002; Clement and Peterson, 2008).

Qualitative temperature reconstructions are available from stable water isotope ($\delta^{18}O$, δD) measurements along polar ice cores. However, quantitative temperature estimates based on the relationship between $\delta^{18}O$ and temperature are limited for Greenland ice due to the influence of precipitation seasonality and source temperature changes (Krinner et al., 1997; Boyle, 1997; Masson-Delmotte et al., 2005). The isotopic composition of nitrogen trapped in air bubbles in the ice quantitatively constrains the magnitude of the fast temperature increases (Severinghaus et al., 1998; Severinghaus and Brook, 1999; Lang et al., 1999). The isotopic composition of nitrogen ($\delta^{15}N$) in the atmosphere is assumed to be essentially constant over time (Mariotti, 1983). Due to gravitational fractionation in the firn column of an ice sheet, $\delta^{15}N$ is increased at the bottom of the firn where air bubbles are enclosed in the ice (lock-in depth) compared to the atmospheric concentration. A rapid temperature increase at the surface of an ice sheet leads to the establishment of a temperature gradient in the firn. Because gases diffuse in the firn about ten times faster than heat, the temperature gradient initiates thermal gas diffusion and leads to a further increase in $\delta^{15}N$ at the lock-in depth compared to the atmospheric value (Severinghaus et al., 1998). This provides a quantitative physical thermometer for fast surface temperature changes on the ice sheet in the past. Neglecting the small difference of diffusion coefficients in air between ^{15}N of N_2 and CH_4, changes in the $\delta^{15}N$ signal in air bubbles enclosed in the ice will have no age difference with respect to CH_4 and are therefore (in contrast to the stable water isotope temperature proxy) ideally suited for studies on phase relationships between temperature and CH_4 (Severinghaus et al., 1998).

Here, we substantially extend and complete the CH_4 record of the NGRIP ice core from the Preboreal Holocene ($\sim$ 10 kyr before present (BP)) back to the end of the last interglacial period ($\sim$ 120 kyr BP). In Sect. 2 the measurement system for CH_4 concentrations is described, and the new and earlier published NGRIP CH_4 data are merged into a consistent concentration scale. In Sect. 3 the new high-resolution CH_4 record from NGRIP is presented and related to the $\delta^{15}N$ data (Kindler et al., 2014; Huber et al., 2006; Landais et al., 2004, 2005; Capron et al., 2010a, b, 2012) and the corresponding NGRIP temperature reconstruction (Kindler et al., 2014). In particular, we compare the magnitude of the CH_4 increases and the NGRIP temperature increases at the onset of DO events and investigate the timing between CH_4 and $\delta^{15}N$ increases. Our discussion in Sect. 4 focuses on the implication of our new results on the evolution of the

wetland CH_4 sources over the last glacial cycle. Conclusions are given in Sect. 5.

2 Methods

At Bern, CH_4 concentrations are determined on air extracted by a melt–refreeze step from ice samples of about 40 g and analyzed by gas chromatography (e.g., Chappellaz et al., 1997; Flückiger et al., 2004). For NGRIP each sample corresponds to a depth interval of about 5 cm. The thermal conductivity detector for the main air components (N_2, O_2 and Ar) and the flame ionization detector for CH_4 are calibrated at hourly intervals with two standard gases (1050 and 408 ppb of CH_4, respectively). Each calibration is checked by a measurement with a third standard gas. The current standard gas is in use since 2010, and a total of 507 standard measurements show a mean concentration with standard deviation of 529.1 ± 3.1 ppb, with no detectable trends over time. Measurements with standard gases from the National Oceanic and Atmospheric Administration (NOAA) show that the Bern scale is approximately 1 % above the NOAA scale. Measurements with air-free ice and standard gas reveal a mean process blank of 10.8 ± 4.6 ppb. This offset is determined for each extraction vessel separately and is subtracted from the measurements on natural ice. Based on the solubilities of the different gases in the melt-water, a negative process blank would be expected. This implies that the expected loss of CH_4 due to solubility is overcompensated by a small CH_4 contamination of unknown origin in the extraction vessels during extraction. Note that the air-free ice produced at the University of Bern may still contain minute amounts of CH_4 potentially leading to an overestimation of the blank correction. Different blank corrections have to be kept in mind when comparing the data from other labs. The precision of the measurements on natural ice is determined by reproducibility measurements of natural ice samples at 22 NGRIP depths. In each of the 22 depths, we measured a series of 5 adjacent samples randomly distributed over the different extraction vessels and duration of the measurement series. The standard deviation of the residuals of the 107 reproducibility samples is 5.9 ppb (1σ). Note that 3 measurements have been excluded due to badly sealed vessels. Note that the measured concentrations are not corrected for the ~ 4 ppb depletion due to gravitational fractionation in the firn column of an ice sheet, in line with previously published work (e.g., Baumgartner et al., 2012; Schilt et al., 2010a, b; Spahni et al., 2005; Huber et al., 2006).

At Laboratoire de Glaciologie et Géophysique de l'Environnement (LGGE) in Grenoble, from where we use a total of 163 previously unpublished NGRIP measurements (carried out in the years 2001–2002), the same technique as in Bern was used but with a standard gas with a CH_4 concentration of 499 ppb (Chappellaz et al., 1997). The LGGE measurements have been performed in parallel to 103 measurements on the Vostok core covering the same climatic period (Bender et al., 2006), which is crucial for a reliable determination of the small interpolar concentration difference (see Sect. 3.4). The standard deviation of the residuals calculated on NGRIP (Vostok) duplicates or triplicates is 2.6 ppb (4.3 ppb).

To check for offsets of the new Bern CH_4 concentrations measurements (performed during the years 2011–2012) compared to previously measured (published or previously unpublished) NGRIP sections, an extensive set of remeasurements has been performed at Bern together with the new measurements. The first part of the previously published data has been analyzed in the years 2002–2004 on the same Bern measurement system (Schilt et al., 2010b; Huber et al., 2006; Flückiger et al., 2004). The second part has been measured at LGGE in the years 2009–2012 (Capron et al., 2010b, 2012). The previously unpublished data from LGGE are from the years 2001–2002 (as mentioned in the preceding paragraph). The remeasurements ensure consistency within the entire NGRIP CH_4 data set, which has been obtained by splicing various different data sets. Amongst others this is crucial for quantification of CH_4 amplitudes at the onset of DO events (see Sect. 3.2). To quantify the offsets in the past we subtract the previously measured concentrations, which are obtained by interpolation to the depth of the Bern remeasurements, from the concentration of the Bern remeasurements (summary in Table 1).

Comparing the Bern measurements, 41 remeasurements are 2.9 ± 1.9 ppb (mean of the residuals and standard error of the mean) higher than measurements performed in 2004. The values published by Huber et al. (2006) are thus consistent with the new data at the 95 % confidence level. 43 remeasurements reveal an offset of 14.5 ± 1.4 ppb compared to measurements performed in 2002 (Flückiger et al., 2004), and 31 remeasurements show an offset of 8.4 ± 2.9 ppb compared to another series of measurements in 2002 (Schilt et al., 2010b). Compared to LGGE Grenoble, 188 remeasurements are 12.2 ± 1.2 ppb higher than the values analyzed during the years 2009–2012 (Capron et al., 2010b, 2012). Since the Bern remeasurements have been measured approximately during the same period (2011–2012) it suggests an increase in the Bern–Grenoble correction compared to the last determined value of 6 ppb (Spahni et al., 2005). Finally, 153 remeasurements are 26.5 ± 1.0 ppb higher than the 163 previously unpublished measurements from LGGE from the years 2001–2002. The reason for this high discrepancy remains unclear, a potential explanation might be the application of a different blank correction at that time.

Based on these remeasurement statistics, we assume a consistent level of Bern concentrations since the year 2004. NGRIP concentrations measured before 2004 (Flückiger et al., 2004; Schilt et al., 2010b) and concentrations from LGGE Grenoble (Capron et al., 2010b, 2012, and previously unpublished data) are increased by the specified values to bring all NGRIP concentrations on a common scale. Note

Table 1. Concentration offsets of new data measured in Bern during the years 2010–2012 compared to previously measured data along the NGRIP ice core. SD and SE denote Standard Deviation and Standard Error, respectively. Offsets are given as new data minus data from reference studies.

Reference study	Climatic period	*n* #	Mean (ppb)	Median (ppb)	SD (ppb)	SE (ppb)	Year of analysis
Huber et al. (2006)	DO 15–17	41	2.9	2.4	12.2	1.9	2004
Schilt et al. (2010b)	T1	31	8.4	8.0	16.1	2.9	2002
Flückiger et al. (2004)	DO 9–12	43	14.5	15.7	9.3	1.4	2002
Capron et al. (2010b, 2012)	DO 23–25	188	12.2	13.0	16.5	1.2	2009–2012
Previously unpublished data LGGE	DO 18–20	153	26.5	26.4	12.4	1.0	2001–2002

that we apply the same analytical precision of 5.9 ppb (1σ), as deduced from the 107 reproducibility measurements of this study, to all the existing NGRIP data. The 10 ppb estimate of previous studies (Chappellaz et al., 1997; Capron et al., 2010b, 2012; Schilt et al., 2010b; Huber et al., 2006; Flückiger et al., 2004), which was based on LGGE reproducibility measurements on artificial air-free ice samples, is therefore replaced by the 5.9 ppb precisely determined from natural ice samples.

3 Results

Figure 1 presents 1094 new CH_4 measurements along the NGRIP ice core. The new measurements cover the time intervals of DO events 5–8, DO events 13–14, and DO events 18–25. Together with the previously published 1008 values (Baumgartner et al., 2012; Capron et al., 2010b, 2012; Schilt et al., 2010b; Huber et al., 2006; Flückiger et al., 2004) this completes the NGRIP record from the Preboreal Holocene back to the end of the last interglacial period (Marine Isotope Stage – MIS – 5.5, also called the Eemian). The mean time resolution of the record is 54 yr, which is in the same order as the width of the gas age distribution of enclosed air in the NGRIP ice core as calculated following Schwander et al. (1993) and Spahni et al. (2003).

The new data set provides the most detailed profile obtained by discrete measurements of the evolution of the CH_4 concentration during the last glacial cycle, and can be compared with continuous CH_4 measurements performed on the North Greenland Eemian Ice Drilling (NEEM) ice core (Chappellaz et al., 2013). It shows that the northern hemisphere CH_4 concentration varied in the range between 360 and 780 ppb during the last glacial cycle (Fig. 2). Apart from the Preboreal Holocene and the end of the Eemian, typical interglacial concentrations of more than 640 ppb are only reached during DO events 17, 21, 23, and 24 (which occur relatively early during the glaciation) and also during the Bølling Allerød (BA). Concentrations of lower than 420 ppb are only reached at the end of the last glacial, in the time period between 30 and 17 kyr BP around the Last Glacial Maximum (LGM). Before that, the Greenland CH_4 concentration never falls below a relatively stable threshold of 420 ppb. In fact, 68 % of all the measurements are found in between 460 and 620 ppb, i.e., within a range of 160 ppb, with the most frequent concentration around 500 ppb (Fig. 2).

3.1 Methane and NGRIP temperature

The CH_4 concentration shows pronounced variations along with Greenland temperature over the last glacial cycle. Here we use the NGRIP temperature (red curve in Fig. 1) as calculated by Kindler et al. (2014), who applied the firn densification and heat diffusion model from Schwander et al. (1997). In brief, the model input parameters, which are the accumulation rate and the temperature based on $\delta^{18}O$ data, were modified until the measured $\delta^{15}N$ could be reproduced by the model. Note that the $\delta^{15}N$ temperature estimate takes into account both the gravitational and thermal fractionation. For more details on the calculation of the temperature record we refer to the companion paper by Kindler et al. (2014).

Figure 1 shows that almost every fast temperature variation has a counterpart in the CH_4 concentration. One exception is found in the temperature peak between DO events 14 and 15, where no CH_4 variation is found, which may be attributed to insufficient data resolution (Huber et al., 2006). Indeed a small CH_4 peak associated with the temperature peak appears in the continuous CH_4 profile on the NEEM ice core (Chappellaz et al., 2013). Similar temperature jumps are associated with different CH_4 amplitudes. A different response to a certain degree of warming is most apparent when comparing DO events 3 and 4. A more quantitative analysis of the amplitudes of the fast temperature and CH_4 increases follows in Sect. 3.2.

During some time periods of slow variations in NGRIP temperature and CH_4 concentration, a decoupling between these two quantities can be observed. During some interstadial periods, e.g., the BA, temperature shows a decreasing trend over several thousand years, while the CH_4 concentration stays at a rather stable level (Fig. 1). A similar pattern is visible during DO events 7 and 22 and during the first part of DO event 8. Decoupling is also visible during certain stadial periods. In the two thousand years before the onset of the BA, the slow increase in the CH_4 concentration occurs at

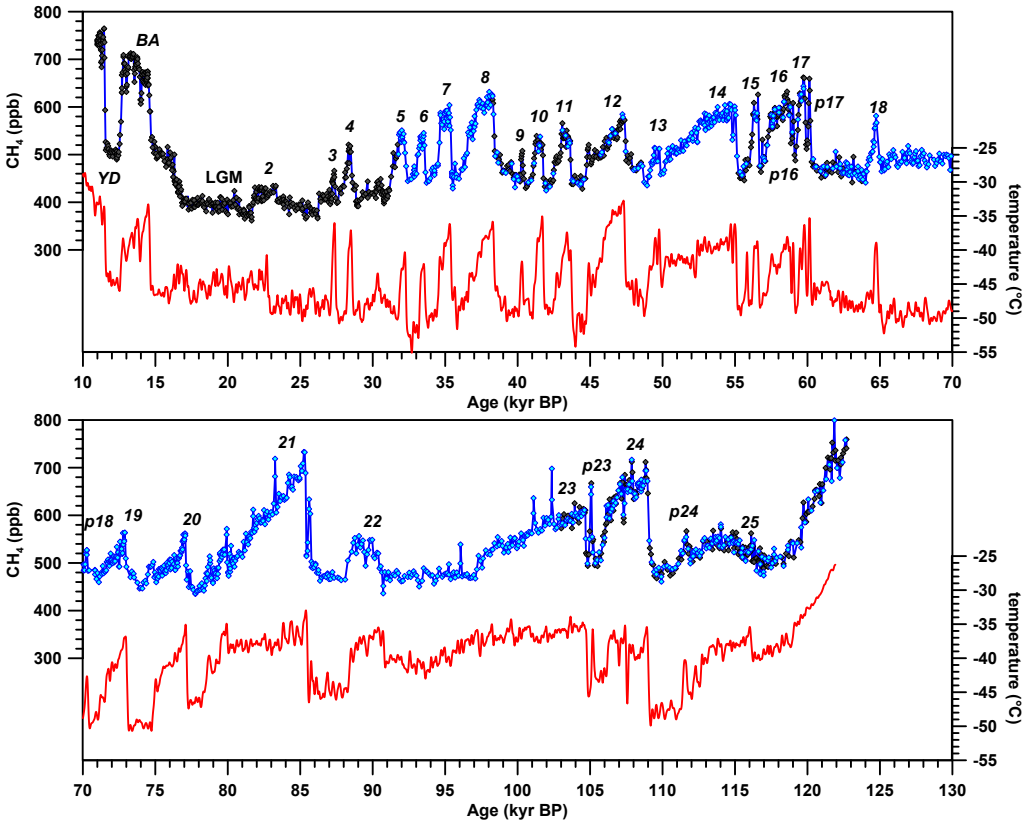

Fig. 1. NGRIP methane and temperature from the Preboreal Holocene back to the end of the last interglacial period. Methane concentrations in black (Baumgartner et al., 2012; Capron et al., 2010b, 2012; Schilt et al., 2010b; Huber et al., 2006; Flückiger et al., 2004) and blue (new data), temperature in red (Kindler et al., 2014). δ^{18}O derived temperature was calibrated by NGRIP δ^{15}N data (Kindler et al., 2014; Huber et al., 2006; Landais et al., 2004, 2005; Capron et al., 2010a, b, 2012). The records are shown on the gas age scale calculated by Kindler et al. (2014) based on the ss09sea06bm ice age scale (NGRIP Project Members, 2004; Andersen et al., 2006; Johnsen et al., 2001). Numbers of DO events are displayed in italics. Short peaks before the main DO events are denoted with a prefix p (e.g., p16).

a stable NGRIP temperature level. In contrast, the slow early CH_4 increases before DO events 8 and 12 are positively correlated with the temperature increases. So while a general synchrony between CH_4 and NGRIP temperature exists for rapid changes, a one-to-one coupling cannot be expected as the temperature record is representative for local temperature changes in Greenland, while CH_4 sources respond to climate changes in boreal and tropical regions.

3.2 Amplitudes of CH_4 and temperature

The clear covariation of the stadial–interstadial CH_4 increases with Greenland temperature increases strongly suggests that CH_4 sources substantially increase emissions connected to a far field response to abrupt northern warming. In the following we investigate how close this tie between North Atlantic/Greenland warming and increases in the CH_4 emissions is. Here, we introduce the ratio μ of CH_4 amplitudes (ΔCH_4) and NGRIP temperature amplitudes (ΔT) for the fast DO event increases as

$$\mu = \frac{\Delta \mathrm{CH_4}}{\Delta T}. \quad (1)$$

μ could be considered an effective CH_4-temperature sensitivity. However, we note that there is not a simple direct influence of temperature changes in Greenland on the CH_4 concentrations. As discussed in detail below, a connection between the two quantities would involve many climate processes in the atmosphere and the ocean which together would lead to changes in the sources and sinks of CH_4 in wetlands. For this reason, we do not use the term henceforth.

ΔCH_4 and ΔT are calculated using spline approximations of the CH_4 data and the temperature reconstruction (Kindler et al., 2014) with cut-off periods of 100 yr. We define empirical thresholds of 0.5 ppb decade^{-1} and 0.05 °C decade^{-1} in the first derivative of the splines as criteria for the start and end points of the fast increases for every onset of a DO event. The amplitude is then calculated in between these two points. Peaks associated with main events or between main events (see Fig. 1) are named as p16, p17, p18, p23, and p24 and are always preceding the main event with the indicated

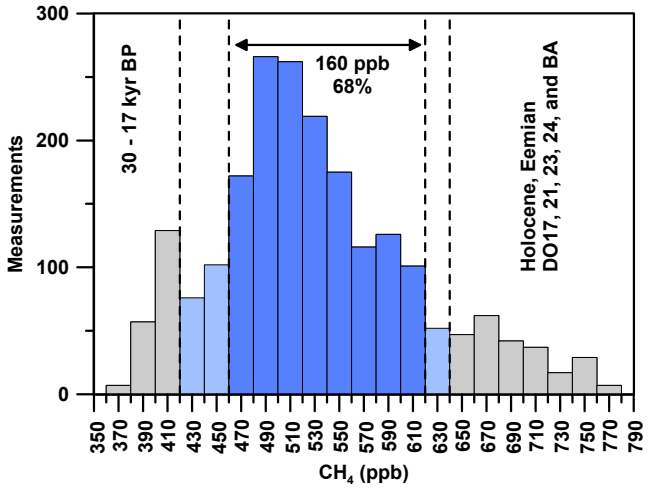

Fig. 2. Histogram of NGRIP methane measurements over the last glacial cycle (120–10 kyr BP). 68 % of all measurements (dark blue) have a concentration between 460 and 620 ppb with the most frequent concentration to be found around 500 ppb. Concentrations below 420 ppb are only found in the time interval between 30 and 17 kyr BP around the LGM. Excluding the Holocene and the end of the Eemian, concentrations higher than 640 ppb occur only in DO events 17, 21, 23, 24, and the BA.

number. Note that the start points of the increases in CH_4 were set manually for DO events 19 and 21, since the data resolution before the increases were lower compared to the cutoff period of the spline. DO events 2 and 25 were excluded from the calculation due to uncertainties in the attribution of the peaks. The results for ΔCH_4, ΔT, and μ for all the other DO events are summarized in Table 2.

Note that μ reflects a covariance of CH_4 concentration amplitudes to temperature amplitudes at the NGRIP site and should not be mixed up with a local temperature sensitivity of CH_4 emissions to the temperature in the wetland source areas. Although for boreal regions the source temperature changes from stadial to interstadial might be smaller than NGRIP temperature changes, they are probably synchronous within few years and correlated in magnitude. A dominant role of the boreal source would thus still lead to relatively stable μ values, but more importantly, μ is a relevant parameter because it documents changes in the Earth system over time (see Sect. 4.2).

Figure 3 shows that CH_4 amplitudes and NGRIP temperature amplitudes are only weakly correlated. Based on the argument above, this basically implies a minor role of the boreal wetland CH_4 sources to the additional emissions from stadial to interstadial. Huber et al. (2006) reported different levels of μ for DO events 9–12 compared to DO events 15–17, while the complete picture of all DO events of the last glacial now suggests that μ varied between ~ 5 and $\sim 18\,\mathrm{ppb\,°C^{-1}}$. Only μ of the transition from the Younger Dryas to the Preboreal Holocene (YD/PB) is with

Table 2. Methane amplitude ΔCH_4 (ppb), temperature amplitude ΔT (°C), and ratio μ ($\mathrm{ppb\,°C^{-1}}$) for the fast increases of DO events. Short peaks before the main DO events are denoted with a prefix p (e.g., p16). Note that the temperature amplitudes are calculated according to the description in Sect. 3.2 and thus might differ compared to the amplitudes calculated by Kindler et al. (2014). Notably this is the case for the DO events, which show a two-step temperature increase (Kindler et al., 2014). In this paper we considered only the fast part of the increases, which better match the fast CH_4 increases.

DO	ΔCH_4 (ppb)	ΔT (°C)	μ ($\mathrm{ppb\,°C^{-1}}$)
0	260.2	10.2	25.5
1	118.2	12.5	9.4
3	63.8	12.6	5.0
4	91.3	12.3	7.4
5	91.6	12.3	7.5
6	100.4	9.3	10.8
7	155.8	11.2	13.9
8	128.7	10.1	12.8
9	75.9	6.3	12.1
10	95.7	13.5	7.1
11	85.9	14.1	6.1
12	87.4	12.6	6.9
13	63.8	8.3	7.6
14	145.9	12.5	11.6
15	148.1	9.7	15.3
16	92.0	6.6	14.0
p16	116.0	10.0	11.6
17	144.0	10.4	13.8
p17	182.7	12.7	14.4
18	113.5	10.1	11.2
p18	44.8	8.3	5.4
19	69.8	13.9	5.0
20	97.4	12.2	8.0
21	222.1	13.5	16.5
22	50.9	5.3	9.6
23	99.3	9.8	10.1
p23	126.6	7.0	18.1
24	177.0	15.0	11.8
p24	41.6	4.8	8.6

$\sim 25.5\,\mathrm{ppb\,°C^{-1}}$ outstandingly high. Apart from the YD/PB, highest μ values are found for DO event 21 and p23, which occurred relatively early during the last glacial. In contrast, the minimum is found for DO event 3, which occurred relatively late during the last glacial. However, DO event 19 and p18 also show similarly low μ values to DO event 3.

3.3 Timing of CH_4 and $\delta^{15}N$

In the following we investigate the phase relationship of the fast temperature and CH_4 increases. Due to the age difference of the ice and the gas at a certain depth (Δage), it is difficult to determine a lead or a lag based on a temperature proxy in

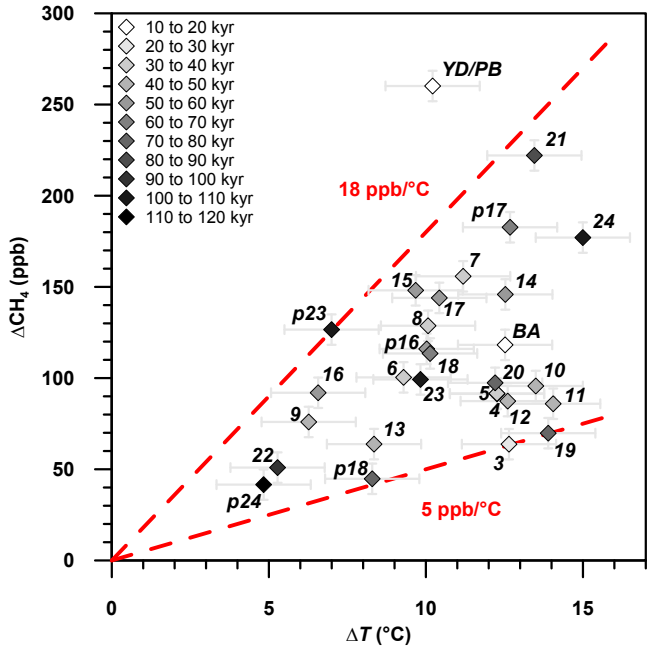

Fig. 3. Comparison of methane and NGRIP temperature amplitudes at the fast DO event increases. The calculations are done as described in Sect. 3.2. Numbers of DO events are displayed in italics. Short peaks before the main DO events are denoted with a prefix p (e.g., p23). The red dashed lines show the envelope defining minimum and maximum μ observed for DO events during the last glacial.

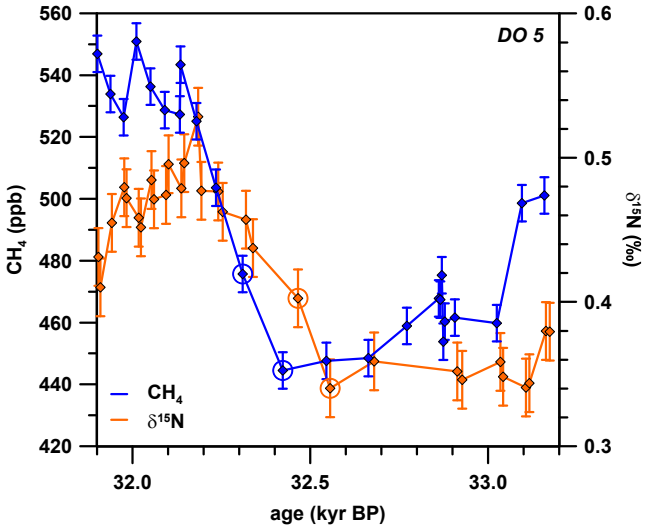

Fig. 4. Timing of CH_4 and $\delta^{15}N$ for DO event 5. CH_4 from NGRIP in blue, $\delta^{15}N$ (Kindler et al., 2014) in orange measured on the same ice core. The selected data points, where the first increase is visible, are indicated by open circles.

the ice phase (water isotopes) and a direct atmospheric parameter stored in the air enclosures in the ice (CH_4). Here, we use the gas phase temperature proxy from stable nitrogen isotopes $\delta^{15}N$ to investigate the timing of the fast temperature and CH_4 increases (Severinghaus et al., 1998). This precludes any uncertainty associated with gas age/ice age differences.

For both, the $\delta^{15}N$ and the CH_4 records, we define the onset of a DO event by the two neighboring data points in between which the first significant increase is visible (see example for DO event 5 in Fig. 4). For both gas proxies, the start of the increase is assumed to be between the ages of the two selected time points ($t_{CH_4,old}$, $t_{CH_4,young}$ for CH_4, $t_{\delta^{15}N,old}$, $t_{\delta^{15}N,young}$ for $\delta^{15}N$), with the most conservative assumption of equal probabilities for all ages within this range. The range of possible lags of CH_4 compared to temperature is then constrained by the two age differences:

$$\mathrm{lag}_{min} = t_{\delta^{15}N,young} - t_{CH_4,old}, \quad (2)$$

$$\mathrm{lag}_{max} = t_{\delta^{15}N,old} - t_{CH_4,young}. \quad (3)$$

The rate of increase between the selected points is always higher than 1.5 ppb decade^{-1} for CH_4 and 0.0018 ‰ decade^{-1} for $\delta^{15}N$. For CH_4, we consider an increase as significant if the concentration difference Δc of the two selected data points is greater than 3σ (i.e., with σ equal to 5.9 ppb such as deduced from our reproducibility test described in Sect. 2; the same criterion is applied for LGGE measurements over DO events 18–20 and 23–25). In case of doubt ($2\sigma < \Delta c < 3\sigma$), we involve a third data point, at the expense of a higher uncertainty range of the starting point. This was the case for the YD/PB and DO events 4, 7, 10, 19, 23, and 24. For $\delta^{15}N$ we use a weaker criterion assuming significant increases if one data point is outside of the uncertainty range of the other data point, because the uncertainty is currently set to 0.02 ‰ (Huber et al., 2006), which is a rather conservative estimate. Again, in case of doubt, a third data point is taken into account. This was the case for the YD/PB and DO events 16 and 18. DO events 2, 3, 22, and 25, as well as p23 and p24, are excluded from the calculations because either the very low amplitude or the noisy baseline before the event made it impossible to attribute the peaks.

We find significant lags of the CH_4 increases compared to temperature increases for DO events 5, 9, 10, 11, 13, 15, 19, and 20, and p18 (see the red curve in Fig. 5 for a cumulative probability density function – pdf). For the remaining events, namely for the YD/PB, the BA, and DO events 4, 6, 7, 8, 12, 14, 16, 17, 18, 21, 23, and 24, as well as peaks p16 and p17, a zero lag is within the equally distributed range of estimated lags (see the black curve in Fig. 5). The results are summarized in Table 3. If we instead just count the DO events for which the last CH_4 sample with stadial concentration precedes the last sample with stadial temperature in $\delta^{15}N$, then this takes place in 4 out of all 25 cases. Accordingly, a lag of CH_4 relative to temperature is more likely than vice versa. For most of the DO events, we can not exclude a small lead of the CH_4 increase, but there exists a clear tendency to lags,

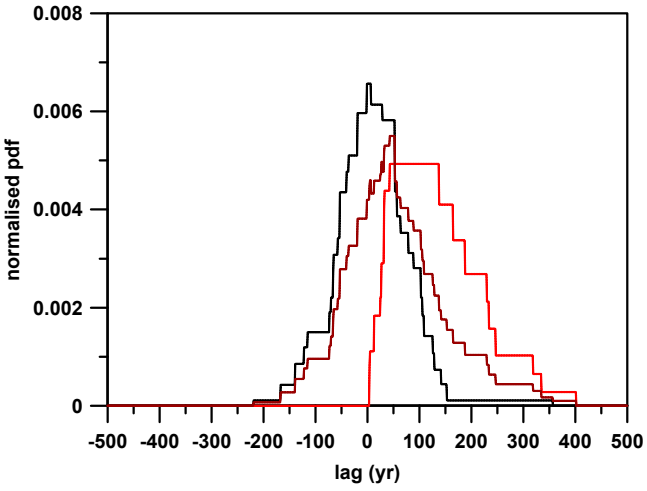

Fig. 5. Normalized probability density function (pdf) of lags between methane and NGRIP temperature for DO events showing a significant lag (red), for DO events showing no significant lag (black), and jointly for all DO events (brown).

with a mean value of 56 ± 19 yr over all DO events (expected value and standard error of the mean from the brown curve in Fig. 5). Note that, although the atmospheric lifetime of CH_4 is relatively short, peak CH_4 concentrations in equilibrium lag a step change in emissions. However, the first increase in concentration essentially starts immediately without a lag. Since we determine the lag at the very beginning of the increase, the effect is negligible.

The pdfs were calculated for three different groups of DO events (red, black, or brown). Inside of the uncertainty range of the lag on the lag axis, the probability of an individual DO event was assumed to be the inverse of the full uncertainty range of the lag. Outside of the uncertainty range of the lag the probability was set to zero. For each group the probabilities of the individual DO events were integrated over the full range of possible lags and normalized to one. Note that the symmetric shape of the pdf for the phase relationship for all DO events is a consequence of our conservative lead/lag estimate. In particular we assume that the true onset of the temperature and CH_4 increase lies anywhere between the two samples defining the respective onsets.

Note that using δ^{15}N data to investigate the timing of Greenland temperature and CH_4 is not straightforward. First, there is a difference in the gas diffusion constants of CH_4 and nitrogen in the firn column. Buizert et al. (2012) (Supplement) specify values for the relative diffusion constants for the NEEM site of 1.367 for CH_4 and 1.275 for nitrogen relative to the diffusion constant of carbon dioxide (CO_2). This implies that CH_4 diffuses 7 % faster than nitrogen, in agreement with Severinghaus et al. (1998). However, since the time of the gas to diffuse through the total firn column is only about 10 yr (Schwander et al., 1993), the difference in the diffusion constant will cause an offset in the order of only 1–3 yr at the very start of the DO event increase and is negligible compared to the uncertainty of the leads and lags we observe. Second, heat conduction in the firn column causes the thermal gradient between the surface and the close-off depth to vanish after a certain time, which is equivalent to the stabilization of the δ^{15}N level at the amount of its gravitational component. However, the thermal conduction in the firn is about 10 times slower than the diffusion of gas. We thus assume that this effect has no influence on the shape of the δ^{15}N signal at the very start of the increase. Third, the δ^{15}N is influenced by the diffusive column height and thus by its gravitational enrichment. Apart from temperature, the diffusive column height is influenced by the accumulation rate of the site (Herron and Langway, 1980). A significant increase in the accumulation rate some hundreds of years before the increase in temperature would increase the diffusive column height and thus increase the gravitational part of δ^{15}N without any change in the temperature. However, on the example of DO event 8, Thomas et al. (2009) showed that the increase in accumulation rate may only occur 2 yr earlier than temperature. Based on their results, we assume that the Greenland accumulation rate and temperature increase occur within a few years for all the DO events, which we consider a reasonable first-order approximation.

3.4 Interpolar difference at 80–60 kyr BP

The 163 previously unpublished NGRIP measurements from LGGE Grenoble have been analyzed together with the samples from the Antarctic Vostok ice core (Bender et al., 2006) within the same measurement campaign and in the same laboratory and cover approximately the same time interval (80–60 kyr BP). This allows us to estimate precisely the interpolar concentration difference (IPD) of CH_4 within this time interval using the same approach as described by Baumgartner et al. (2012). Figure 6 shows that the fast increases of DO events 18, 19, and 20 can be identified in both the NGRIP and the Vostok data, which defines tie points for CH_4 synchronization. However, in between these sharp DO events, no further events suitable as CH_4 tie points are found.

We do not estimate a peak interstadial rIPD during the very short DO events 18, 19, and 20, since the attenuation of the atmospheric variation due to the slow bubble enclosure process (Spahni et al., 2003) is much stronger in the Vostok ice core compared to the NGRIP ice core. If the NGRIP data are attenuated according to the conditions of the firn at the Vostok site (light blue line in Fig. 6 is the output from the firn model, Schwander et al., 1993; Spahni et al., 2003), the amplitudes of the three DO events are substantially reduced. Estimates of temperature and accumulation rate at the Vostok site between 80 and 60 kyr BP, which are important parameters in the firn model regarding the gas enclosure process, are taken from Petit et al. (1999) and Siegert (2003).

Table 3. Depth interval [d_{young}, d_{old}], time interval [t_{young}, t_{old}], and lag interval [lag_{min}, lag_{max}] calculated from Eqs. (2) and (3) at the start of the fast increases in CH_4 and $\delta^{15}N$ at the onset of DO events. Short peaks before the main DO events are denoted with a prefix p (e.g., p16).

DO	$d_{CH_4,young}$ (m)	$d_{CH_4,old}$ (m)	$d_{\delta^{15}N,young}$ (m)	$d_{\delta^{15}N,old}$ (m)	$t_{CH_4,young}$ (yr)	$t_{CH_4,old}$ (yr)	$t_{\delta^{15}N,young}$ (yr)	$t_{\delta^{15}N,old}$ (yr)	lag_{min} (yr)	lag_{max} (yr)
0	1518.0	1519.7	1517.5	1519.8	11 533.2	11 585.7	11 519.4	11 589.9	−66	57
1	1631.3	1633.0	1631.4	1634.7	14 653.5	14 711.3	14 657.7	14 778.6	−54	125
4	1912.9	1914.6	1913.6	1915.0	28 572.5	28 682.7	28 611.9	28 714.2	−71	142
5	1974.0	1975.1	1975.5	1976.3	32 309.8	32 422.7	32 465.5	32 555.9	43	246
6	1996.0	1997.1	1995.0	1996.1	33 642.3	33 721.5	33 581.9	33 649.1	−140	7
7	2029.0	2031.2	2029.3	2030.1	35 387.3	35 525.1	35 402.6	35 450.7	−122	63
8	2088.0	2088.4	2087.7	2089.8	38 400.8	38 424.4	38 383.6	38 509.3	−41	109
9	2117.5	2119.2	2119.6	2120.5	40 435.8	40 560.9	40 592.8	40 669.1	32	233
10	2140.6	2142.3	2142.7	2144.6	41 748.9	41 875.3	41 908.1	42 083.5	33	335
11	2173.0	2174.2	2174.5	2176.6	43 654.0	43 730.5	43 754.5	43 972.1	24	318
12	2236.4	2236.9	2236.6	2237.1	47 459.5	47 496.5	47 476.5	47 512.0	−20	52
13	2269.3	2270.4	2270.7	2271.7	49 792.5	49 873.4	49 899.5	49 980.0	26	188
14	2357.9	2358.9	2357.1	2358.2	55 144.4	55 245.3	55 077.7	55 173.2	−168	29
15	2377.7	2378.8	2379.1	2380.2	56 591.9	56 685.3	56 717.0	56 821.2	32	229
16	2410.1	2410.7	2409.9	2411.9	58 815.0	58 859.6	58 802.5	58 943.4	−57	128
p16	2413.4	2414.0	2413.2	2414.2	59 051.2	59 110.1	59 037.0	59 130.2	−73	79
17	2425.5	2426.1	2425.3	2426.3	59 869.5	59 910.4	59 856.6	59 922.5	−54	53
p17	2431.6	2432.7	2431.9	2432.8	60 203.2	60 294.1	60 228.4	60 309.2	−66	106
18	2474.4	2476.1	2474.0	2477.3	64 772.1	64 963.6	64 743.7	65 128.2	−220	356
p18	2515.1	2515.7	2515.8	2516.2	70 277.4	70 356.6	70 368.7	70 442.0	12	165
19	2542.3	2543.7	2543.7	2545.5	72 897.3	73 003.7	73 008.1	73 298.3	4	401
20	2586.1	2586.6	2586.6	2587.3	77 121.8	77 167.1	77 170.9	77 259.6	4	138
21	2692.3	2693.4	2693.3	2693.9	85 365.7	85 429.7	85 428.0	85 468.1	−2	102
23	2896.0	2897.2	2896.9	2897.4	104 696.8	104 820.2	104 783.7	104 849.2	−36	152
24	2945.2	2946.1	2945.3	2945.8	109 121.3	109 245.8	109 130.8	109 209.7	−115	88

For the stadials, we calculate the IPD (rIPD) as a mean over the time interval between two sharp DO event peaks, which yields 20.7 ± 3.0 ppb (4.6 ± 0.7 %) for the stadial between DO events 18 and 19 and 19.6 ± 3.7 ppb (4.4 ± 0.8 %) for the stadial between DO events 19 and 20. Between DO events 17 and 18 the IPD (rIPD) appears to be lower 11.2 ± 5.8 ppb (2.6 ± 1.4 %) but has a relatively high uncertainty because the NGRIP data from LGGE cover half of the stadial only, which introduces a high synchronization uncertainty of the first NGRIP data point to the Vostok record. A rIPD reconstruction before DO event 20 is not possible since the time resolution of the Vostok record over DO event 21 does not permit a precise synchronization. Note that by taking mean IPD values over rather long periods, potential short periods of very low rIPD around 64, 70, and 74 kyr BP are not considered. Two of those appear to have higher IPD values after taking the attenuation into account, while the third example around 70 kyr BP would need additional information on synchronization to make more detailed statements.

4 Discussion

The discussion focuses on the implication of our results on the evolution of the wetland CH_4 sources over the last glacial cycle. The new NGRIP CH_4 record is compared to CH_4 records from Antarctica in Sect. 4.1, and the variations in the ratio of CH_4 amplitudes to NGRIP temperature amplitudes μ are discussed in Sect. 4.2. Finally, Sect. 4.3 discusses the timing of CH_4 and NGRIP temperature.

4.1 Information from the interpolar difference

The CH_4 concentrations reconstructed from Greenland and Antarctica are different by some percent, which yields valuable information on the latitudinal distribution of the CH_4 sources (Fig. 7b). Baumgartner et al. (2012) found a relatively stable positive rIPD of about 3–7 % around the LGM (32–11 kyr BP, in green) and revised the zero rIPD estimate from Dällenbach et al. (2000) during the LGM. The rIPD results between 80 and 60 kyr BP (in green) from the NGRIP and Vostok ice cores presented in this study (Sect. 3.4) show relatively small rIPD of the same order as the values

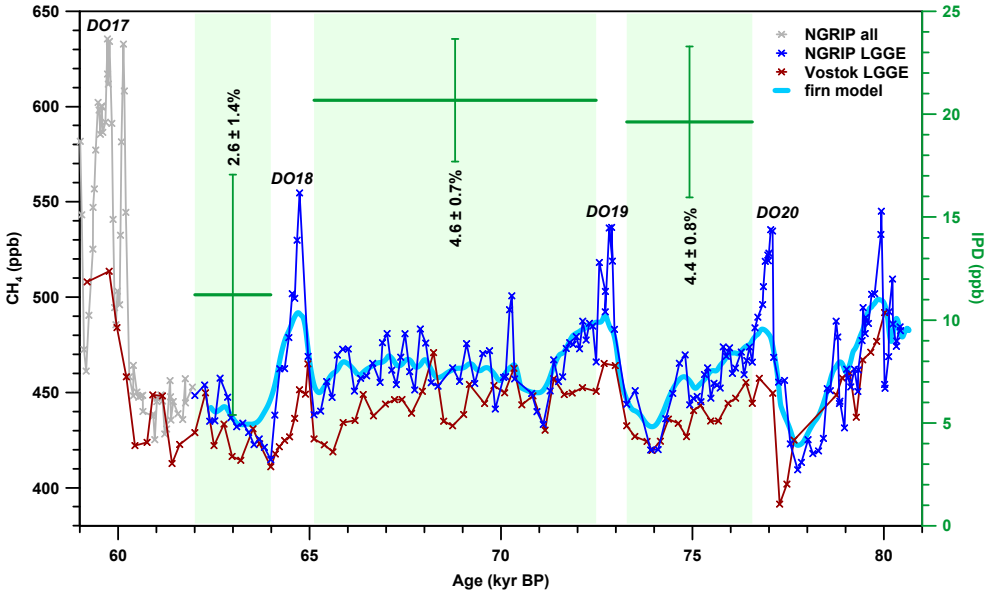

Fig. 6. Interpolar concentration difference of methane calculated in the stadial periods between 80 and 60 kyr BP. The samples from Greenland (new data from NGRIP in blue) and Vostok (red, Bender et al., 2006) have been measured during the same measurement series and in the same laboratory (LGGE Grenoble). The absolute interpolar concentration difference (IPD) is shown in green, the relative interpolar concentration difference (rIPD) is given in numbers. The methane data from NGRIP that are not from LGGE and shown in grey (new data and Huber et al., 2006) are shifted to the LGGE scale in this plot (see Sect. 2 for details to the offset corrections). The thick blue line represents the firn model output (Schwander et al., 1993; Spahni et al., 2003), where the NGRIP data have been attenuated to Vostok conditions.

from Baumgartner et al. (2012) pointing to a similar source distribution as during the LGM.

For DO events 3–12, Dällenbach et al. (2000) suggested a relative increase of the northern source compared to the southern source from stadial to interstadial based on the rIPD. Here, we merge the existing ice core CH_4 data from EPICA Dronning Maud Land (EDML) (Baumgartner et al., 2012; Capron et al., 2010b; EPICA Community Members, 2006; Schilt et al., 2010b) and Talos Dome Ice Core (TALDICE) (Buiron et al., 2011; Stenni et al., 2011; Schilt et al., 2010b) (red curve in Fig. 7a) and look at the rIPD based on this combined Antarctic record and our new NGRIP record from Greenland (blue curve in Fig. 7a). The published records from EDML and TALDICE have been corrected for the 6 ppb offset between Bern and LGGE (Spahni et al., 2005); however, comparison of all available data reveals remaining mean interlaboratory offsets of another 6.2 ± 1.2 ppb for TALDICE, and 6.4 ± 1.0 ppb for EDML for ages younger than 50 kyr BP and 11.9 ± 0.8 ppb for ages older than 50 kyr BP. We applied these additional offset corrections to put all values on the Bern reference scale and note that, apart from EDML for ages older than 50 kyr BP, the total offset corrections are well in line with the 12.7 ± 1.1 ppb offset derived from recently measured NGRIP data at Bern and LGGE over DO events 23–25 (see Sect. 2). Very short events, whose amplitudes could have been affected differently by varying attenuation characteristics at the different sites (Spahni et al., 2003; Baumgartner et al., 2012), are excluded. Note that our new NGRIP CH_4 data reveal that the AICC2012 (Veres et al., 2013) gas age scale for NGRIP is inconsistent with the CH_4 data of EDML and TALDICE for several DO event transitions. We thus do not make use of the AICC2012 but use our own CH_4 synchronization.

In the mean over all the remaining DO events, we qualitatively confirm the statement from Dällenbach et al. (2000) and support a northward shift of the CH_4 sources during the transition from stadial (blue) to interstadial (red) conditions. However, the rIPD as calculated from NGRIP, EDML and TALDICE does not show a continuous reduction over the last glacial cycle as might be expected from the growth of the ice sheets and the associated suppression of the boreal source strength. Note that we refrain from making more detailed statements due to the offsets between the different NGRIP sections (see Sect. 2) and also due to offsets between measurements of Bern and LGGE in the EDML and the TALDICE records. We underline the necessity of analyzing in the future both Greenland and Antarctic ice core samples during one joint measurement campaign to be able to derive reliable rIPD values as recently performed by Baumgartner et al. (2012), Mitchell et al. (2013) or in this study over DO events 18–20 (Sect. 3.4).

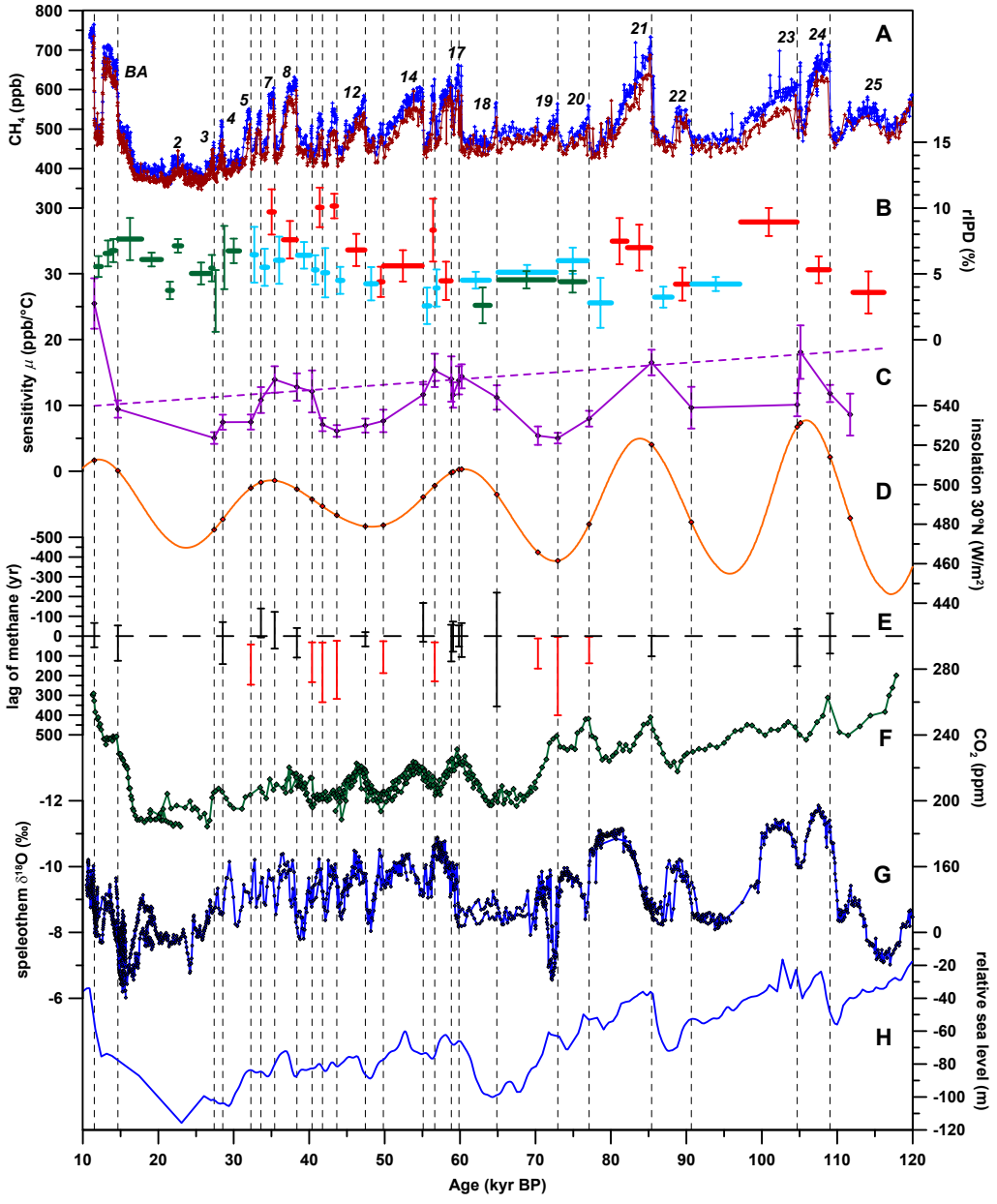

Fig. 7. Variations in μ and timing of the fast DO event increases. **(A)** Atmospheric CH_4 concentration from NGRIP (blue, Baumgartner et al., 2012; Capron et al., 2010b, 2012; Schilt et al., 2010b; Huber et al., 2006; Flückiger et al., 2004, and new data) and merged records from EDML (Baumgartner et al., 2012; Schilt et al., 2010b; Capron et al., 2010b; EPICA Community Members, 2006) and TALDICE (Buiron et al., 2011; Stenni et al., 2011; Schilt et al., 2010b) ice cores in red; **(B)** rIPD from Baumgartner et al. (2012) and new data from this study over DO events 18–20 in green, rIPD (after application of offset corrections) based on NGRIP and merged EDML and TALDICE in red (interstadial) and blue (stadial); **(C)** ratio μ of CH_4 amplitudes to NGRIP temperature amplitudes, the dashed line is the regression through the maxima of μ; **(D)** 6 June insolation evaluated at the ages of the DO events (orange diamonds) at 30° N (Quinn et al., 1991); **(E)** lag of the fast CH_4 concentration increases and NGRIP temperature increase as it is visible in the comparison of CH_4 and $\delta^{15}N$ (Kindler et al., 2014), the events marked with red show lags significantly different from zero; **(F)** atmospheric CO_2 concentration from EDML and TALDICE (Bereiter et al., 2012; Lüthi et al., 2010), EPICA Dome C (Monnin et al., 2001), and the Byrd ice core (Ahn and Brook, 2007, 2008); **(G)** speleothem $\delta^{18}O$ from Hulu and Sanbao cave (Wang et al., 2001, 2008), Hulu cave values are shifted by +1.6‰ to match the Sanbao values (Wang et al., 2008); **(H)** smoothed version of the sea level record (Rohling et al., 2009; Grant et al., 2012). Speleothem and sea level records are shown on their original timescales, the other records are on the gas age scale calculated by Kindler et al. (2014) based on the ss09sea06bm ice age scale (NGRIP Project Members, 2004; Andersen et al., 2006; Johnsen et al., 2001). The CO_2 records have been brought on the same age scale by CH_4 synchronization – see **(A)**.

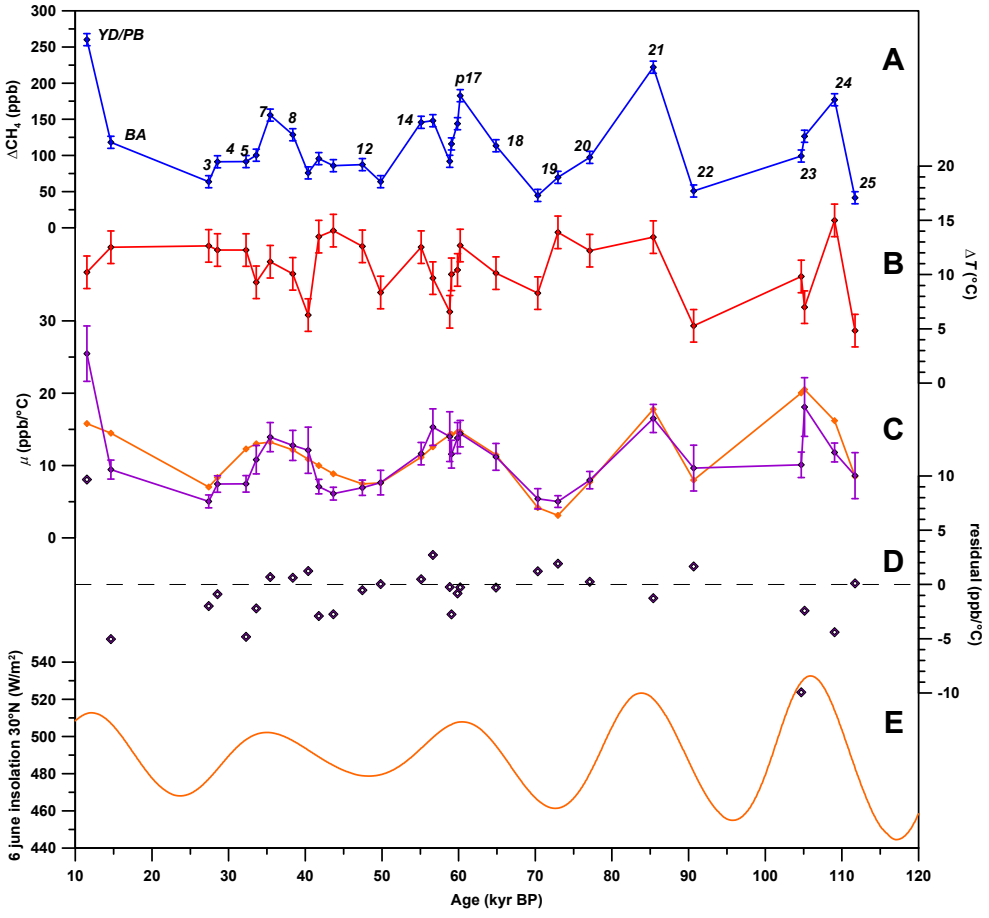

Fig. 8. Normalization of insolation to the μ scale. **(A)** CH_4 amplitudes at DO events from NGRIP (see also Fig. 3); **(B)** Greenland temperature amplitudes at DO events from NGRIP; **(C)** μ (purple line, see also Fig. 7c) and 6 June insolation at 30° N normalized to the μ scale (orange); **(D)** residuals of μ minus normalized 6 June insolation at 30° N; **(E)** 6 June insolation at 30° N.

4.2 Variations in μ

The ratio μ of CH_4 amplitudes to NGRIP temperature amplitudes at the fast DO warmings (Figs. 7c and 8c) shows covariation to northern low-latitude summer insolation (Fig. 7d and Fig. 8e). This covariance with insolation is also visible in the CH_4 DO event amplitudes alone (Fig. 8a) (Flückiger et al., 2004; Brook et al., 1996).

Based on the connection of CH_4 amplitudes with low-latitude northern summer insolation, Flückiger et al. (2004) concluded that the seasonal distribution of insolation is crucial for wetland CH_4 emission strength at the onset of DO events. The precessional influence is also visible in cave speleothem $\delta^{18}O$ records (Fig. 7g), a proxy for monsoon strength in northern mid-latitudes (Wang et al., 2001, 2008). Apparently, the rapid Greenland DO event temperature variations have counterparts in mid-latitude precipitation records, which implies a far-field influence of extratropical warming on these important CH_4 wetland regions (Chiang and Friedman, 2012). The fast increases in precipitation are in connection with latitudinal shifts of the Intertropical Convergence Zone (ITCZ) and the monsoon systems (Chiang, 2009; Broccoli et al., 2006; Bozbiyik et al., 2011), which moves the necessary amount of moisture from the southern to the CH_4-source rich northern mid-latitudes. Variations in the amount of precipitation (e.g., monsoon strength) from one DO event to the other are thus very likely to drive the observed non-linear variations in μ via total wetland area and length of emission seasons.

Temperature changes at the onset of DO events reconstructed from NGRIP (Kindler et al., 2014) and used for the calculation of μ reflect changes in Greenland mean annual temperatures from stadial to interstadial conditions. In contrast, most important for wetland CH_4 productivity is the averaged temperature at the wetland source location during the warmest months of the year. The amplitude of the seasonal temperature variation, i.e., maximum annual temperature minus mean annual temperature, depends on the amplitude of the seasonal variation in insolation at a given latitude. While the stadial CH_4 baseline does not appear to be strongly modulated by insolation, it is the evolution of the peak interstadial

concentrations that leads to the covariance of the CH_4 amplitudes and northern summer insolation (Flückiger et al., 2004). Thus the non-linear variations in μ could be supported by variations in the difference of maximum annual temperature minus mean annual temperature at mid-latitude wetland source locations during interstadial periods.

From 120 to 20 kyr BP we observe an overall decrease in the maxima of μ, indicated by the dashed regression line in Fig. 7c. Looking at the insolation curve it is notable that the local maxima in northern summer insolation decrease in parallel to the maxima in μ. Following the argument above, the decrease of the maxima in μ could be a consequence of decreasing wetland extent and/or decreasing summer temperature relative to mean annual temperature at the northern low latitude CH_4 source regions. The lack of DO events around the insolation minima at 96 and 117 kyr BP makes it impossible to compare the trend of the μ minima with the insolation minima over the full last glacial. However, the minimum of μ around 72 kyr BP appears to be lower than the minimum around 48 kyr BP, which is in line with the increase in the two corresponding insolation minima. We therefore conclude that insolation alone is able to explain a very large part of the variability in μ.

Figure 8c shows 6 June insolation at 30° N normalized to the μ scale (orange curve). Note that 6 June insolation was chosen because it shows the highest correlation ($R = 0.72$) to μ (purple curve). In Fig. 8d the normalized insolation is subtracted from μ and the corresponding residuals are shown to discuss potential minor effects in the variability of μ that are not driven by insolation. Note that the residuals can potentially be affected by age scale uncertainties. Potential candidates, which could influence wetland CH_4 emissions are the CO_2 concentration (Fig. 7f, Bereiter et al., 2012; Lüthi et al., 2010; Ahn and Brook, 2007, 2008; Monnin et al., 2001) or sea level (Fig. 7h, Rohling et al., 2009; Grant et al., 2012). Sea level is certainly a candidate that can alter total wetland area. Probably most importantly, a higher sea level leads to a higher ground water level and thus promotes the existence of wet areas at coastal low lands. CO_2 on the other hand influences the net primary productivity and thus is important to provide organic material, which can be decomposed to CH_4 (Bridgham et al., 2013).

The range of μ (5.0–25.5 ppb °C^{-1}) obtained from our data compares well to an experiment from a wetland CH_4 emission model simulation (6.3–24.1 ppb °C^{-1}) by Hopcroft et al. (2011), who applied different idealized climate states. Hopcroft et al. (2014) performed a similar experiment for the BA, p17, and DO events 8 and 11, resulting in sensitivities of 12.2, 11.5, 9.6, and 8.5 ppb °C^{-1}, respectively. The deviation from our μ values for the specified events is +29, −10, +57, and −41 %, respectively. Hopcroft et al. (2011, 2014) notice that their model generally underestimates the total CH_4 amplitudes; however, it also underestimates the Greenland temperature variations calculated from a freshwater hosing experiment. The largest deviations are found for DO event 11 and p17, which occur around extreme northern summer insolation states (Fig. 7d). In comparison, the deviations during DO event 8 and the BA, which occur during moderate northern summer insolation states, are smaller. Although the different insolation states are taken into account by Hopcroft et al. (2014), it is possible that the influence of northern summer insolation has to be refined in the model.

4.3 Timing of CH_4 and NGRIP temperature

Figure 7e shows the timing of the fast NGRIP temperature and CH_4 increases for all considered DO events, with the events showing a significant lag displayed in red. Our reconstruction for DO event 21 is consistent with Vallelonga et al. (2012), who also used the gas phase temperature proxy $\delta^{15}N$ to compare with high-resolution CH_4 data on NGRIP ice and estimated a maximum lag for this event of 69 ± 5 yr with a most probable lag of only a few decades. The processes that could lead to a lag of the CH_4 increases compared to NGRIP temperature increases at the onset of DO events are not well understood. One can think of two extreme CH_4 source evolution scenarios leading to a lag of CH_4. In the first case, where the stadial CH_4 sources are maintained after the start of Greenland warming, all the important additional CH_4 sources causing the stadial–interstadial concentration increase must be delayed by at least the time of the corresponding lag. Otherwise, if there were any important additional sources showing an immediate response to Greenland warming, we would expect the CH_4 concentration to achieve at least parts of its DO event increase instantaneously. In the second case a breakdown of parts of the stadial CH_4 sources immediately after the Greenland warming leads to the reduction in emissions compensated by the rapid response of the new sources. Due to the short atmospheric lifetime of CH_4, this process of source compensation would create a lag between the start of the increase in atmospheric CH_4 concentration relative to the start of the increase in emissions of the interstadial CH_4 sources. In the following we will discuss why we think the second scenario is more likely.

Modeling studies suggest an immediate increase in Northern Hemisphere temperature as a reaction to high-latitude northern warming (e.g., Menviel et al., 2011; Renold et al., 2010). Accordingly, an immediate response of the existing CH_4 wetland source regions would be expected in agreement with the majority of the DO events (Fig. 7e, black). An immediate response of boreal wetland CH_4 sources to a rapid cooling is also supported in a North Atlantic freshwater hosing experiment by a dynamic vegetation model study (Zürcher et al., 2013). A recent global CH_4 wetland emission model study simulates slightly different temporal evolutions of tropical compared to boreal wetland CH_4 source responses to a DO event warming (Ringeval et al., 2013), but the global increase starts when the first source increases, which is at the same time as the Greenland temperature increase in the same model run (Hopcroft et al., 2011).

On the other hand, the concept of latitudinal shifts in the position of the ITCZ at stadial–interstadial transitions (e.g., Bozbiyik et al., 2011; Chiang, 2009; Chiang and Friedman, 2012; Chiang et al., 2003; Wang et al., 2004), which is visible in the speleothem records (Fig. 7g, Wang et al., 2001, 2008), supports a replacement of the stadial by new interstadial CH_4 source regions driven by the displacement of the precipitation belts that feed the wetlands. A northward shift of the CH_4 sources is also supported by our rIPD reconstruction (Fig. 7b) for most of the DO events. Based on the rIPD a particularly strong northward shift is expected for DO events 10–11, which are two of those events showing a significant lag compared to NGRIP temperature. The two-box model from Baumgartner et al. (2012) indeed predicts a $\sim 50\,\%$ decrease in the southern hemispheric source strength from stadial to interstadial for such a rIPD configuration, which requires compensation by new source regions before the fast DO event increase of the CH_4 concentrations can start. Looking at CH_4 increase rates, Chappellaz et al. (2013) find maximum increase rates for DO events during the last glacial of 0.6–2.5 ppb yr^{-1} based on CH_4 measurements from continuous flow analysis along the NEEM ice core. In line with the theory of source compensation, the events showing a significant lag belong to the group of smaller increase rates. It is further apparent that, with the exception of DO event 15, the CH_4 amplitudes of the events showing a lag are relatively small, which means that the orbital configuration was favorable for southern hemispheric emissions before the onset of the DO event (Flückiger et al., 2004). Losing the southern emissions due to northern warming by drastic source replacement could contribute to the very low amplitudes. A drastic replacement of stadial CH_4 sources could further support a lag of CH_4 by the time needed to transform existing vegetation to wetlands at the new source locations and also to thaw permafrost at high boreal regions. In this context one might argue that a high lag of CH_4 compared to Greenland temperature implies a more drastic latitudinal dislocation of the CH_4 source regions and unfavorable conditions for CH_4 emissions in the Southern Hemisphere.

5 Conclusions

We have presented new high-resolution CH_4 measurements, which complete and extend the NGRIP record from the Preboreal Holocene back to the end of the last interglacial period. We related the amplitudes of the CH_4 increases at the onset of DO events to a temperature record measured along the same ice core (Kindler et al., 2014). The ratio μ of CH_4 amplitudes to NGRIP temperature amplitudes shows variations between 5 and 18 ppb $°C^{-1}$ along with the precessional cycle likely due to variations in temperature or wetland extent at the northern low latitude source regions. Calculation of the timing of CH_4 and NGRIP temperature, where we used a δ^{15}N-based temperature reconstruction (Kindler et al., 2014; Huber et al., 2006; Landais et al., 2004, 2005; Capron et al., 2010a, b, 2012), has revealed a tendency to lags of the CH_4 increases of about 56 ± 19 yr on average. We hypothesize that the DO events showing a higher lag are characterized by stronger northward shifts of the source regions, in line with generally low CH_4 increase rates. Bottom-up emissions models, which incorporate the processes of ITCZ shifts and transformation from vegetation to wetland area, might be able to simulate the temporal evolution of CH_4 emissions at a DO event transition. We have shown that the rIPD of CH_4, which is a further important constraint for modeling studies, is about 4.5 % in the stadials between DO events 18 and 20, which compares well with the rIPD before and after DO event 2 (Baumgartner et al., 2012). The rIPD tends to be higher for interstadials compared to stadials and does not show obvious trends during the glacial, but future bipolar measurements are required to confirm and extend the rIPD estimates over DO events 5–17 and DO events 21–25.

Supplementary material related to this article is available online at http://www.clim-past.net/10/903/2014/cp-10-903-2014-supplement.zip.

Acknowledgements. This work, which is a contribution to the North Greenland Ice Core Project (NGRIP), was supported by the University of Bern, the Swiss National Science Foundation, and the Prince Albert II of Monaco Foundation. Additional support was provided by the LEFE program of CNRS/INSU. NGRIP is coordinated by the Department of Geophysics at the Niels Bohr Institute for Astronomy, Physics and Geophysics, University of Copenhagen. It is supported by Funding Agencies in Denmark (SHF), Belgium (FNRS-CFB), France (IPEV and INSU/CNRS), Germany (AWI), Iceland (RannIs), Japan (MEXT), Sweden (SPRS), Switzerland (SNF) and the United States of America (NSF, Office of Polar Programs). The research leading to these results has received funding from the European Union's Seventh Framework program (FP7/2007–2013) under grant agreement no. 243908, Past4Future. Climate change – Learning from the past climate. This is Past4Future contribution no. 71.

Edited by: E. Brook

References

Ahn, J. and Brook, E. J.: Atmospheric CO_2 and climate from 65 to 30 ka BP, Geophys. Res. Lett., 34, L10703, doi:10.1029/2007GL029551, 2007.

Ahn, J. and Brook, E. J.: Atmospheric CO_2 and climate on millennial time scales during the last glacial period, Science, 322, 83–85, doi:10.1126/science.1160832, 2008.

Andersen, K. K., Svensson, A., Johnsen, S. J., Rasmussen, S. O., Bigler, M., Röthlisberger, R., Ruth, U., Siggaard-Andersen, M.-L., Steffensen, J. P., Dahl-Jensen, D., Vinther, B. M., and Clausen, H. B.: The Greenland ice core chronology 2005, 15–42 ka, Part 1: Constructing the time scale, Quaternary Sci. Rev., 25, 3246–3257, doi:10.1016/j.quascirev.2006.08.002, 2006.

Baumgartner, M., Schilt, A., Eicher, O., Schmitt, J., Schwander, J., Spahni, R., Fischer, H., and Stocker, T. F.: High-resolution interpolar difference of atmospheric methane around the Last Glacial Maximum, Biogeosciences, 9, 3961–3977, doi:10.5194/bg-9-3961-2012, 2012.

Bender, M. L., Floch, G., Chappellaz, J., Suwa, M., Barnola, J.-M., Blunier, T., Dreyfus, G., Jouzel, J., and Parrenin, F.: Gas age–ice age differences and the chronology of the Vostok ice core, 0–100 ka, J. Geophys. Res., 111, D21115, doi:10.1029/2005JD006488, 2006.

Bereiter, B., Lüthi, D., Siegrist, M., Schüpbach, S., Stocker, T. F., and Fischer, H.: Mode change of millennial CO_2 variability during the last glacial cycle associated with a bipolar marine carbon seesaw, P. Natl. Acad. Sci. USA, 109, 9755–9760, doi:10.1073/pnas.1204069109, 2012.

Bloom, A. A., Palmer, P. I., Fraser, A., Reay, D. S., and Frankenberg, C.: Large-scale controls of methanogenesis inferred from methane and gravity spaceborne data, Science, 327, 322–325, doi:10.1126/science.1175176, 2010.

Boyle, E. A.: Cool tropical temperatures shift the global δ^{18}O-T relationship: an explanation for the ice core δ^{18}O-borehole thermometry conflict?, Geophys. Res. Lett., 24, 273–276, doi:10.1029/97GL00081, 1997.

Bozbiyik, A., Steinacher, M., Joos, F., Stocker, T. F., and Menviel, L.: Fingerprints of changes in the terrestrial carbon cycle in response to large reorganizations in ocean circulation, Clim. Past, 7, 319–338, doi:10.5194/cp-7-319-2011, 2011.

Bridgham, S. D., Cadillo-Quiroz, H., Keller, J. K., and Zhuang, Q.: Methane emissions from wetlands: biogeochemical, microbial, and modeling perspectives from local to global scales, Global Change Biol., 19, 1325–1346, doi:10.1111/gcb.12131, 2013.

Broccoli, A. J., Dahl, K. A., and Stouffer, R. J.: Response of the ITCZ to Northern Hemisphere cooling, Geophys. Res. Lett., 33, L01702, doi:10.1029/2005GL024546, 2006.

Brook, E., Sowers, T., and Orchardo, J.: Rapid variations in atmospheric methane concentration during the past 110 000 years, Science, 273, 1087–1091, doi:10.1126/science.273.5278.1087, 1996.

Brook, E. J., Harder, S., Severinghaus, J., Steig, E. J., and Sucher, C. M.: On the origin and timing of rapid changes in atmospheric methane during the last glacial period, Global Biogeochem. Cy., 14, 559–572, doi:10.1029/1999GB001182, 2000.

Buiron, D., Chappellaz, J., Stenni, B., Frezzotti, M., Baumgartner, M., Capron, E., Landais, A., Lemieux-Dudon, B., Masson-Delmotte, V., Montagnat, M., Parrenin, F., and Schilt, A.: TALDICE-1 age scale of the Talos Dome deep ice core, East Antarctica, Clim. Past, 7, 1–16, doi:10.5194/cp-7-1-2011, 2011.

Buizert, C., Martinerie, P., Petrenko, V. V., Severinghaus, J. P., Trudinger, C. M., Witrant, E., Rosen, J. L., Orsi, A. J., Rubino, M., Etheridge, D. M., Steele, L. P., Hogan, C., Laube, J. C., Sturges, W. T., Levchenko, V. A., Smith, A. M., Levin, I., Conway, T. J., Dlugokencky, E. J., Lang, P. M., Kawamura, K., Jenk, T. M., White, J. W. C., Sowers, T., Schwander, J., and Blunier, T.: Gas transport in firn: multiple-tracer characterisation and model intercomparison for NEEM, Northern Greenland, Atmos. Chem. Phys., 12, 4259–4277, doi:10.5194/acp-12-4259-2012, 2012.

Capron, E., Landais, A., Chappellaz, J., Schilt, A., Buiron, D., Dahl-Jensen, D., Johnsen, S. J., Jouzel, J., Lemieux-Dudon, B., Loulergue, L., Leuenberger, M., Masson-Delmotte, V., Meyer, H., Oerter, H., and Stenni, B.: Millennial and sub-millennial scale climatic variations recorded in polar ice cores over the last glacial period, Clim. Past, 6, 345–365, doi:10.5194/cp-6-345-2010, 2010a.

Capron, E., Landais, A., Lemieux-Dudon, B., Schilt, A., Masson-Delmotte, V., Buiron, D., Chappellaz, J., Dahl-Jensen, D., Johnsen, S., Leuenberger, M., Loulergue, L., and Oerter, H.: Synchronising EDML and NorthGRIP ice cores using δ^{18}O of atmospheric oxygen (δ^{18}O (atm)) and CH_4 measurements over MIS5 (80–123 kyr), Quaternary Sci. Rev., 29, 222–234, doi:10.1016/j.quascirev.2009.07.014, 2010b.

Capron, E., Landais, A., Chappellaz, J., Buiron, D., Fischer, H., Johnsen, S. J., Jouzel, J., Leuenberger, M., Masson-Delmotte, V., and Stocker, T. F.: A global picture of the first abrupt climatic event occurring during the last glacial inception, Geophys. Res. Lett., 39, L15703, doi:10.1029/2012GL052656, 2012.

Chappellaz, J., Blunier, T., Kints, S., Dällenbach, A., Barnola, J. M., Schwander, J., Raynaud, D., and Stauffer, B.: Changes in the atmospheric CH_4 gradient between Greenland and Antarctica during the Holocene, J. Geophys. Res.-Atmos., 102, 15987–15997, 1997.

Chappellaz, J., Stowasser, C., Blunier, T., Baslev-Clausen, D., Brook, E. J., Dallmayr, R., Faïn, X., Lee, J. E., Mitchell, L. E., Pascual, O., Romanini, D., Rosen, J., and Schüpbach, S.: High-resolution glacial and deglacial record of atmospheric methane by continuous-flow and laser spectrometer analysis along the NEEM ice core, Clim. Past, 9, 2579–2593, doi:10.5194/cp-9-2579-2013, 2013.

Chiang, J. C.: The tropics in Paleoclimate, Annu. Rev. Earth Pl. Sc., 37, 263–297, doi:10.1146/annurev.earth.031208.100217, 2009.

Chiang, J. C. and Friedman, A. R.: Extratropical cooling, interhemispheric thermal gradients, and tropical climate change, Annu. Rev. Earth Pl. Sc., 40, 383–412, doi:10.1146/annurev-earth-042711-105545, 2012.

Chiang, J. C. H., Biasutti, M., and Battisti, D.: Sensitivity of the Atlantic Intertropical Convergence Zone to Last Glacial Maximum boundary conditions, Paleoceanography, 18, 1094, doi:10.1029/2003PA000916, 2003.

Christensen, T. R., Ekberg, A., Ström, L., Mastepanov, M., Panikov, N., Öquist, M., Svensson, B. H., Nykänen, H., Martikainen, P. J., and Oskarsson, H.: Factors controlling large scale variations in methane emissions from wetlands, Geophys. Res. Lett., 30, 1414, doi:10.1029/2002GL016848, 2003.

Clement, A. C. and Peterson, L. C.: Mechanisms of abrupt climate change of the last glacial period, Rev. Geophys., 46, RG4002, doi:10.1029/2006RG000204, 2008.

Dällenbach, A., Blunier, T., Flückiger, J., Stauffer, B., Chappellaz, J., and Raynaud, D.: Changes in the atmospheric CH_4 gradient between Greenland and Antarctica during the Last Glacial and the transition to the Holocene, Geophys. Res. Lett., 27, 1005–1008, 2000.

Dansgaard, W., Clausen, H. B., Gundestrup, N., Hammer, C. U., Johnsen, S. F., Kristinsdottir, P. M., and Reeh, N.: A new Greenland deep ice core, Science, 218, 1273–1277, doi:10.1126/science.218.4579.1273, 1982.

EPICA Community Members: One-to-one coupling of glacial climate variability in Greenland and Antarctica, Nature, 444, 195–198, 2006.

Etheridge, D. M., Steele, L. P., Francey, R. J., and Langenfelds, R. L.: Atmospheric methane between 1000 AD and present: evidence of anthropogenic emissions and climatic variability, J. Geophys. Res.-Atmos., 103, 15979–15993, doi:10.1029/98JD00923, 1998.

Flückiger, J., Blunier, T., Stauffer, B., Chappellaz, J., Spahni, R., Kawamura, K., Schwander, J., Stocker, T. F., and Dahl-Jensen, D.: N_2O and CH_4 variations during the last glacial epoch: insight into global processes, Global Biogeochem. Cy., 18, GB1020, doi:10.1029/2003GB002122, 2004.

Grant, K. M., Rohling, E. J., Bar-Matthews, M., Ayalon, A., Medina-Elizalde, M., Ramsey, C. B., Satow, C., and Roberts, A. P.: Rapid coupling between ice volume and polar temperature over the past 150 000 years, Nature, 491, 744–747, doi:10.1038/nature11593, 2012.

Hartmann, D. L., Klein Tank, A. M. G., Rusticucci, M., Alexander, L. V., Brönnimann, S., Charabi, Y., Dentener, F. J., Dlugokencky, E. J., Easterling, D. R., Kaplan, A., Soden, B. J., Thorne, P. W., Wild, M., and Zhai, P. M.: Observations: Atmosphere and Surface. In: Climate Change 2013: The Physical Science Basis. Contribution of Working Group I to the Fifth Assessment Report of the Intergovernmental Panel on Climate Change, edited by: Stocker, T. F., Qin, D., Plattner, G.-K., Tignor, M., Allen, S. K., Boschung, J., Nauels, A., Xia, Y., Bex, V., and Midgley, P. M., Cambridge University Press, Cambridge, UK and New York, NY, USA, 2013.

Herron, M. M. and Langway, C. C.: Firn densification – an empirical-model, J. Glaciol., 25, 373–385, 1980.

Hopcroft, P. O., Valdes, P. J., and Beerling, D. J.: Simulating idealized Dansgaard–Oeschger events and their potential impacts on the global methane cycle, Quaternary Sci. Rev., 30, 3258–3268, doi:10.1016/j.quascirev.2011.08.012, 2011.

Hopcroft, P. O., Valdes, P. J., Wania, R., and Beerling, D. J.: Limited response of peatland CH_4 emissions to abrupt Atlantic Ocean circulation changes in glacial climates, Clim. Past, 10, 137–154, doi:10.5194/cp-10-137-2014, 2014.

Huber, C., Leuenberger, M., Spahni, R., Flückiger, J., Schwander, J., Stocker, T. F., Johnsen, S., Landais, A., and Jouzel, J.: Isotope calibrated Greenland temperature record over Marine Isotope Stage 3 and its relation to CH_4, Earth Planet. Sc. Lett., 243, 504–519, 2006.

Johnsen, S. J., Dahl-Jensen, D., Gundestrup, N., Steffensen, J. P., Clausen, H., Miller, H., Masson-Delmotte, V., Sveinbjornsdottir, A., and White, J.: Oxygen isotope and palaeotemperature records from six Greenland ice-core stations: Camp Century, Dye-3, GRIP, GISP2, Renland and NorthGRIP, J. Quaternary Sci., 16, 299–307, 2001.

Kindler, P., Guillevic, M., Baumgartner, M., Schwander, J., Landais, A., and Leuenberger, M.: Temperature reconstruction from 10 to 120 kyr b2k from the NGRIP ice core, Clim. Past, 10, 887–902, doi:10.5194/cp-10-887-2014, 2014.

Krinner, G., Genthon, C., and Jouzel, J.: GCM analysis of local influences on ice core delta signals, Geophys. Res. Lett., 24, 2825–2828, doi:10.1029/97GL52891, 1997.

Landais, A., Barnola, J. M., Masson-Delmotte, V., Jouzel, J., Chappellaz, J., Caillon, N., Huber, C., Leuenberger, M., and Johnsen, S. J.: A continuous record of temperature evolution over a sequence of Dansgaard–Oeschger events during marine isotopic stage 4 (76 to 62 kyr BP), Geophys. Res. Lett., 31, L22211, doi:10.1029/2004GL021193, 2004.

Landais, A., Jouzel, J., Masson-Delmotte, V., and Caillon, N.: Large temperature variations over rapid climatic events in Greenland: a method based on air isotopic measurements, C. R. Geosci., 337, 947–956, doi:10.1016/j.crte.2005.04.003, 2005.

Lang, C., Leuenberger, M., Schwander, J., and Johnsen, S.: 16 °C rapid temperature variation in Central Greenland 70 000 years ago, Science, 286, 934–937, doi:10.1126/science.286.5441.934, 1999.

Levine, J. G., Wolff, E. W., Jones, A. E., Sime, L. C., Valdes, P. J., Archibald, A. T., Carver, G. D., Warwick, N. J., and Pyle, J. A.: Reconciling the changes in atmospheric methane sources and sinks between the Last Glacial Maximum and the pre-industrial era, Geophys. Res. Lett., 38, L23804, doi:10.1029/2011GL049545, 2011.

Levine, J. G., Wolff, E. W., Hopcroft, P. O., and Valdes, P. J.: Controls on the tropospheric oxidizing capacity during an idealized Dansgaard–Oeschger event, and their implications for the rapid rises in atmospheric methane during the last glacial period, Geophys. Res. Lett., 39, L12805, doi:10.1029/2012GL051866, 2012.

Li, C., Battisti, D. S., and Bitz, C. M.: Can North Atlantic sea ice anomalies account for Dansgaard–Oeschger climate signals?, J. Climate, 23, 5457–5475, doi:10.1175/2010JCLI3409.1, 2010.

Loulergue, L., Schilt, A., Spahni, R., Masson-Delmotte, V., Blunier, T., Lemieux, B., Barnola, J.-M., Raynaud, D., Stocker, T. F., and Chappellaz, J.: Orbital and millennial-scale features of atmospheric CH_4 over the past 800 000 years, Nature, 453, 383–386, doi:10.1038/nature06950, 2008.

Lüthi, D., Bereiter, B., Stauffer, B., Winkler, R., Schwander, J., Kindler, P., Leuenberger, M., Kipfstuhl, S., Capron, E., Landais, A., Fischer, H., and Stocker, T. F.: CO_2 and O_2/N_2 variations in and just below the bubble-clathrate transformation zone of Antarctic ice cores, Earth Planet. Sc. Lett., 297, 226–233, doi:10.1016/j.epsl.2010.06.023, 2010.

Mariotti, A.: Atmospherig nitrogen is a reliable standard for natural ^{15}N abundance measurements, Nature, 303, 685–687, doi:10.1038/303685a0, 1983.

Masson-Delmotte, V., Jouzel, J., Landais, A., Stievenard, M., Johnsen, S. J., White, J. W. C., Werner, M., Sveinbjornsdottir, A., and Fuhrer, K.: GRIP Deuterium Excess Reveals Rapid and Orbital-Scale Changes in Greenland Moisture Origin, Science, 309, 118–121, doi:10.1126/science.1108575, http://www.sciencemag.org/content/309/5731/118.abstract, 2005.

McManus, J. F., Francois, R., Gherardi, J. M., Kegwin, L. D., and Brown-Leger, S.: Collapse and rapid resumption of Atlantic meridional circulation linked to deglacial climate changes, Nature, 428, 834–837, 2004.

Melton, J. R., Wania, R., Hodson, E. L., Poulter, B., Ringeval, B., Spahni, R., Bohn, T., Avis, C. A., Beerling, D. J., Chen, G., Eliseev, A. V., Denisov, S. N., Hopcroft, P. O., Lettenmaier, D. P., Riley, W. J., Singarayer, J. S., Subin, Z. M., Tian, H., Zürcher, S., Brovkin, V., van Bodegom, P. M., Kleinen, T., Yu, Z. C., and Kaplan, J. O.: Present state of global wetland extent and wetland methane modelling: conclusions from a model inter-comparison project (WETCHIMP), Biogeosciences, 10, 753–788, doi:10.5194/bg-10-753-2013, 2013.

Menviel, L., Timmermann, A., Timm, O. E., and Mouchet, A.: Deconstructing the Last Glacial termination: the role of millennial and orbital-scale forcings, Quaternary Sci. Rev., 30, 1155–1172, doi:10.1016/j.quascirev.2011.02.005, 2011.

Mitchell, L., Brook, E., Lee, J. E., Buizert, C., and Sowers, T.: Constraints on the Late Holocene Anthropogenic Contribution to the Atmospheric Methane Budget, Science, 342, 964–966, doi:10.1126/science.1238920, 2013.

Monnin, E., Indermühle, A., Dällenbach, A., Flückiger, J., Stauffer, B., Stocker, T. F., Raynaud, D., and Barnola, J.-M.: Atmospheric CO_2 concentrations over the Last Glacial termination, Science, 291, 112–114, doi:10.1126/science.291.5501.112, 2001.

NGRIP Project Members: High-resolution record of Northern Hemisphere climate extending into the last interglacial period, Nature, 431, 147–151, 2004.

Petersen, S. V., Schrag, D. P., and Clark, P. U.: A new mechanism for Dansgaard–Oeschger cycles, Paleoceanography, 28, 24–30, doi:10.1029/2012PA002364, 2013.

Petit, J., Jouzel, J., Raynaud, D., Barkov, N., Barnola, J., Basile, I., Bender, M., Chappellaz, J., Davis, M., Delaygue, G., Delmotte, M., Kotlyakov, V., Legrand, M., Lipenkov, V., Lorius, C., Pepin, L., Ritz, C., Saltzman, E., and Stievenard, M.: Climate and atmospheric history of the past 420,000 years from the Vostok ice core, Antarctica, Nature, 399, 429–436, doi:10.1038/20859, 1999.

Piotrowski, A. M., Goldstein, S. L., Hemming, S. R., and Fairbanks, R. G.: Intensification and variability of ocean thermohaline circulation through the last deglaciation, Earth Planet. Sc. Lett., 225, 205–220, doi:10.1016/j.epsl.2004.06.002, 2004.

Prather, M. J., Holmes, C. D., and Hsu, J.: Reactive greenhouse gas scenarios: Systematic exploration of uncertainties and the role of atmospheric chemistry, Geophys. Res. Lett., 39, L09803, doi:10.1029/2012GL051440, 2012.

Quinn, T., Tremaine, S., and Duncan, M.: A 3 million year integration of the Earths orbit, Astron. J., 101, 2287–2305, 1991.

Renold, M., Raible, C. C., Yoshimori, M., and Stocker, T. F.: Simulated resumption of the North Atlantic meridional overturning circulation – slow basin-wide advection and abrupt local convection, Quaternary Sci. Rev., 29, 101–112, doi:10.1016/j.quascirev.2009.11.005, 2010.

Ringeval, B., Hopcroft, P. O., Valdes, P. J., Ciais, P., Ramstein, G., Dolman, A. J., and Kageyama, M.: Response of methane emissions from wetlands to the Last Glacial Maximum and an idealized Dansgaard–Oeschger climate event: insights from two models of different complexity, Clim. Past, 9, 149–171, doi:10.5194/cp-9-149-2013, 2013.

Rohling, E. J., Grant, K., Bolshaw, M., Roberts, A. P., Siddall, M., Hemleben, C., and Kucera, M.: Antarctic temperature and global sea level closely coupled over the past five glacial cycles, Nat. Geosci., 2, 500–504, doi:10.1038/ngeo557, 2009.

Schilt, A., Baumgartner, M., Blunier, T., Schwander, J., Spahni, R., Fischer, H., and Stocker, T. F.: Glacial-interglacial and millennial-scale variations in the atmospheric nitrous oxide concentration during the last 800 000 years, Quaternary Sci. Rev., 29, 182–192, 2010a.

Schilt, A., Baumgartner, M., Schwander, J., Buiron, D., Capron, E., Chappellaz, J., Loulergue, L., Schüpbach, S., Spahni, R., Fischer, H., and Stocker, T. F.: Atmospheric nitrous oxide during the last 140 000 years, Earth Planet. Sc. Lett., 300, 33–43, 2010b.

Schwander, J., Barnola, J. M., Andrie, C., Leuenberger, M., Ludin, A., Raynaud, D., and Stauffer, B.: The age of the air in the firn and the ice at Summit, Greenland, J. Geophys. Res.-Atmos., 98, 2831–2838, 1993.

Schwander, J., Sowers, T., Barnola, J., Blunier, T., Fuchs, A., and Malaize, B.: Age scale of the air in the summit ice: implication for glacial-interglacial temperature change, J. Geophys. Res.-Atmos., 102, 19483–19493, doi:10.1029/97JD01309, 1997.

Severinghaus, J. P. and Brook, E. J.: Abrupt climate change at the end of the Last Glacial period inferred from trapped air in Polar ice, Science, 286, 930–934, doi:10.1126/science.286.5441.930, 1999.

Severinghaus, J. P., Sowers, T., Brook, E. J., Alley, R. B., and Bender, M. L.: Timing of abrupt climate change at the end of the Younger Dryas interval from thermally fractionated gases in polar ice, Nature, 391, 141–146, doi:10.1038/34346, 1998.

Siegert, M.: Glacial-interglacial variations in central East Antarctic ice accumulation rates, Quaternary Sci. Rev., 22, 741–750, doi:10.1016/S0277-3791(02)00191-9, 2003.

Spahni, R., Schwander, J., Flückiger, J., Stauffer, B., Chappellaz, J., and Raynaud, D.: The attenuation of fast atmospheric CH_4 variations recorded in polar ice cores, Geophys. Res. Lett., 30, 1571, doi:10.1029/2003GL017093, 2003.

Spahni, R., Chappellaz, J., Stocker, T. F., Loulergue, L., Hausammann, G., Kawamura, K., Flückiger, J., Schwander, J., Raynaud, D., Masson-Delmotte, V., and Jouzel, J.: Atmospheric methane and nitrous oxide of the Late Pleistocene from Antarctic ice cores, Science, 310, 1317–1321, doi:10.1126/science.1120132, 2005.

Spahni, R., Wania, R., Neef, L., van Weele, M., Pison, I., Bousquet, P., Frankenberg, C., Foster, P. N., Joos, F., Prentice, I. C., and van Velthoven, P.: Constraining global methane emissions and uptake by ecosystems, Biogeosciences, 8, 1643–1665, doi:10.5194/bg-8-1643-2011, 2011.

Stenni, B., Buiron, D., Frezzotti, M., Albani, S., Barbante, C., Bard, E., Barnola, J. M., Baroni, M., Baumgartner, M., Bonazza, M., Capron, E., Castellano, E., Chappellaz, J., Delmonte, B., Falourd, S., Genoni, L., Iacumin, P., Jouzel, J., Kipfstuhl, S., Landais, A., Lemieux-Dudon, B., Maggi, V., Masson-Delmotte, V., Mazzola, C., Minster, B., Montagnat, M., Mulvaney, R., Narcisi, B., Oerter, H., Parrenin, F., Petit, J. R., Ritz, C., Scarchilli, C., Schilt, A., Schüpbach, S., Schwander, J., Selmo, E., Severi, M., Stocker, T. F., and Udisti, R.: Expression of the bipolar see-saw in Antarctic climate records during the last deglaciation, Nat. Geosci., 4, 46–49, 2011.

Stocker, T. F. and Johnsen, S. J.: A minimum thermodynamic model for the bipolar seesaw, Paleoceanography, 18, 1087, doi:10.1029/2003PA000920, 2003.

Thomas, E. R., Wolff, E. W., Mulvaney, R., Johnsen, S. J., Steffensen, J. P., and Arrowsmith, C.: Anatomy of a Dansgaard–Oeschger warming transition: high-resolution analysis of the North Greenland Ice Core Project ice core, J. Geophys. Res., 114, D08102, doi:10.1029/2008JD011215, 2009.

Vallelonga, P., Bertagna, G., Blunier, T., Kjær, H. A., Popp, T. J., Rasmussen, S. O., Steffensen, J. P., Stowasser, C., Svensson, A. S., Warming, E., Winstrup, M., Bigler, M., and Kipfstuhl, S.: Duration of Greenland Stadial 22 and ice-gas Δage from counting of annual layers in Greenland NGRIP ice core, Clim. Past, 8, 1839–1847, doi:10.5194/cp-8-1839-2012, 2012.

Veres, D., Bazin, L., Landais, A., Toyé Mahamadou Kele, H., Lemieux-Dudon, B., Parrenin, F., Martinerie, P., Blayo, E., Blunier, T., Capron, E., Chappellaz, J., Rasmussen, S. O., Severi, M., Svensson, A., Vinther, B., and Wolff, E. W.: The Antarctic ice core chronology (AICC2012): an optimized multi-parameter and multi-site dating approach for the last 120 thousand years, Clim. Past, 9, 1733–1748, doi:10.5194/cp-9-1733-2013, 2013.

Voelker, A. H.: Global distribution of centennial-scale records for Marine Isotope Stage (MIS) 3: a database, Quaternary Sci. Rev., 21, 1185–1212, doi:10.1016/S0277-3791(01)00139-1, 2002.

Walter, B. P., Heimann, M., and Matthews, E.: Modeling modern methane emissions from natural wetlands: 1. Model description and results, J. Geophys. Res.-Atmos., 106, 34189–34206, doi:10.1029/2001JD900165, 2001.

Wang, X., Auler, A., Edwards, R., Cheng, H., Cristalli, P., Smart, P., Richards, D., and Shen, C.: Wet periods in northeastern Brazil over the past 210 kyr linked to distant climate anomalies, Nature, 432, 740–743, doi:10.1038/nature03067, 2004.

Wang, Y. J., Cheng, H., Edwards, R. L., An, Z. S., Wu, J. Y., Shen, C. C., and Dorale, J. A.: A high-resolution absolute-dated Late Pleistocene monsoon record from Hulu Cave, China, Science, 294, 2345–2348, 2001.

Wang, Y. J., Cheng, H., Edwards, R. L., Kong, X., Shao, X., Chen, S., Wu, J., Jiang, X., Wang, X., and An, Z.: Millennial- and orbital-scale changes in the East Asian monsoon over the past 224 000 years, Nature, 451, 1090–1093, doi:10.1038/nature06692, 2008.

Wania, R., Melton, J. R., Hodson, E. L., Poulter, B., Ringeval, B., Spahni, R., Bohn, T., Avis, C. A., Chen, G., Eliseev, A. V., Hopcroft, P. O., Riley, W. J., Subin, Z. M., Tian, H., Brovkin, V., van Bodegom, P. M., Kleinen, T., Yu, Z. C., Singarayer, J. S., Zürcher, S., Lettenmaier, D. P., Beerling, D. J., Denisov, S. N., Prigent, C., Papa, F., and Kaplan, J. O.: Present state of global wetland extent and wetland methane modelling: methodology of a model intercomparison project (WETCHIMP), Geosci. Model Dev., 6, 617–641, doi:10.5194/gmd-6-617-2013, 2013.

Zürcher, S., Spahni, R., Joos, F., Steinacher, M., and Fischer, H.: Impact of an abrupt cooling event on interglacial methane emissions in northern peatlands, Biogeosciences, 10, 1963–1981, doi:10.5194/bg-10-1963-2013, 2013.